Self-Assembling Peptide−Polymer Conjugates Comprising (D-*alt*-L)-Cyclopeptides as Aggregator Domains

Mattijs G. J. ten Cate,[†] Nikolai Severin,[‡] and Hans G. Börner*,[†]

Max Planck Institute of Colloids and Interfaces, MPI KGF Golm, 14424 Potsdam, Germany, and Department of Physics, Humboldt University Berlin, Newtonstrasse 15, 12489 Berlin, Germany

Received August 1, 2006; Revised Manuscript Received September 7, 2006

ABSTRACT: The synthesis of peptide−polymer conjugates comprising (D-*alt*-L)-cyclopeptides as aggregator domains and their self-assembly into tubelike structures is described. By coupling two well-defined poly(*n*-butyl acrylate) blocks to opposite sides of a preformed cyclic (D-*alt*-L)-α-octapeptide, a coil−ring−coil bioconjugate was accessed. The applied solution-phase coupling route allowed a multigram scale synthesis of the conjugate and assured both a controlled synthesis and ease of analysis. The controlled self-assembly of the conjugate leads to uniform tube structures. Atomic force microscopy (AFM) of these aggregates deposited on mica revealed a height of 1.4 ± 0.2 nm, a width of 5 nm, and roughly estimated lengths of up to 200−300 nm. A model is proposed, explaining the structure dimensions. This includes the formation of a tubular peptide core build via stacking of the cyclopeptides and a poly(*n*-butyl acrylate) shell wrapping around the peptide tube. The model is consistent with infrared spectroscopy and electron diffraction measurements, verifying that the peptide segment of the conjugate adopts a β-sheet structure, similar to unsubstituted (D-*alt*-L)-cyclopeptides. Hence, the stacks of peptide rings are stabilized along the fiber axis via inter-ring β-sheet H-bonding. The tube structures are capable to interact laterally, organizing further into weak networks as was evidenced by AFM and transmission electron microscopy.

Introduction

Peptide−polymer conjugates showing self-assembly properties allow to access an interesting class of structured bio-(mimetic) materials, prospectively exhibiting the potentials for diverse applications from nanotechnology to tissue engineering.[1−9] This arises from their ability to self-assemble into well-defined nanostructures,[10−14] combined, on one hand, with a remarkable control of chemical functionalities and, on the other hand, potentials to actively interact with biological systems.[15,16] Sequence controlled oligopeptides that self-assemble, in a spontaneous manner or in a triggered way, into strongly anisometric nanostructures such as tapes, filaments, or fibers have been investigated intensively.[8,9,17−21] It was shown that the formation of β-sheet secondary structure motif is essential for the self-assembly into these structures.[18] Hence, for robust assemblies, peptides with high propensity to adopt a stable β-sheet are required. Recently, an universal route was demonstrated by utilizing very short peptide strands that were preorganized via an organic template. This preorganization adjusts peptide segments into the appropriate β-sheet geometry and restricts the conformational freedom compared to linear peptide strands. The resulting peptide clamp showed a strongly enhanced tendency to form antiparallel β-sheets compared to the linear analogues.[8,20] This route allows one to obtain stable structures, while using comparatively small peptides, and thus, the amount of the expensive peptide segments can be reduced relative to the polymer.

Further development of this approach leads directly to cyclic peptides with small ring sizes, exhibiting an even stronger reduction of the conformational freedom. Thus, the loss of conformational entropy during aggregation is expected to be smaller, making them potentially more suitable as strong aggregators.

An elegant design of cyclic peptides with self-assembling properties was introduced by Ghadiri et al., who used a peptide sequence of alternating D- and L-α-amino acids. Cyclic peptides composed of an even number of amino acids with alternating chirality, in combination with rather small ring sizes of 8 or 12 amino acids, adopt in average flat, ring-shaped conformations.[14,22] It might be noteworthy that such planar ring conformations are usually not favored by cyclopeptides that consist entirely of amino acids with the same chirality (either D or L). However, a high tendency of (D-*alt*-L)-peptide rings can be observed to assemble into tubular ring stacks.[14,22] Such peptide nanotubes are formed due to anisotropy of the ring structure[23] and stabilization occurs by β-sheet-like hydrogen-bonding between antiparallel oriented cyclic peptides.[14,22,24,25] In this structure the H-bonds of the β-sheet are following the tube growth axis and the side chains of the amino acid moieties are directed outward. Therefore, the resulting peptide nanotubes are showing a functionalizable exterior and a hollow interior that allows, e.g., depending on the ring size of the peptide cycles, a passive transport of substrates based on size exclusion.[26−28]

Compared to the β-sheet of linear peptides, the hydrogen bonding between the different ring-unimers in a tubular structure is considered to be rather specific (Figure 1). Conformational defects during aggregation process are prevented by design, because the precise geometry and spacing of the H-bond acceptors and donors at the tube termini allow only binding in the case of an accurate fit. A defect, such as a small shift of the peptide cycle during aggregation, results in a dramatic decrease of the number of hydrogen bonds, leading to an unstable structure, and hence the aggregation of the peptide cycles potentially show auto-correction. This is in strong contrast to, e.g., the β-sheet formation of linear peptides, where a shift of a β-strand may lead to a loss of a very small proportion of

* To whom correspondence should be addressed. E-mail: hans.boerner@mpikg.mpg.de. Telephone: 0049-(0)331-567-9552. Fax: 0049-(0)331-567-9502.
[†] Max Planck Institute of Colloids and Interfaces, MPI KGF Golm.
[‡] Department of Physics, Humboldt University Berlin.

10.1021/ma061738p CCC: $33.50
Published on Web 10/19/2006

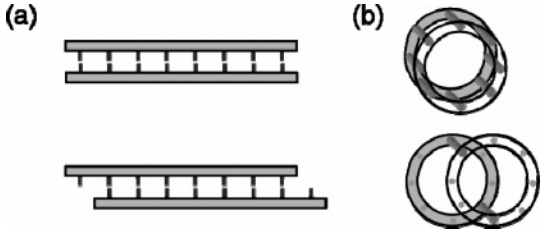

Figure 1. Schematic illustration of H-bonding between linear (a) and cyclic peptide β-strands (b): ideal fit resulting in maximum H-bonds (top) and a slight mismatch (bottom).

hydrogen bonds as outlined in Figure 1a. This capability of molecular recognition based on geometry fixation of donor and acceptor H-binding sides makes it possible for the (D-*alt*-L)-peptide cycles to highly interesting organizer domains to be exploited for peptide-guided microstructure formation of synthetic polymers. Moreover, the resulting nanotubes[29−36] are appealing structural elements.[26,37,38]

Recently it was demonstrated that self-assembled peptide nanotubes can be used as scaffolds to graft polymers to the exterior of pre-assembled tubes.[39] This was accomplished by cyclic (D-*alt*-L)-peptides which were modified with three initiation sides for atom-transfer radical polymerization (ATRP[40,41]) per peptide cycle. These were self-assembled into nanotubes and subsequently used to graft *N*-isopropylacrylamide. However, the tube surface contained a high density of initiator groups that might cause ring−ring cross-linking due to radical recombination in the early, uncontrolled stage of the ATRP process. Moreover, the high density of growing polymer chains leads to partial dissociation of the nanotubes, since a reduction of the tube lengths from 100−500 nm of the nongrafted tubes to 60−100 nm of the polymer coated tubes was described.[39] This is also consistent with the literature, showing the rupture of even C−C bonds in molecular bottle brushes, in the case of a too high density of side chain grafts.[42]

Therefore, a different approach was used, synthesizing well-defined building blocks that can be characterized as nonaggregated unimers. The subsequent organization of these building blocks in a controlled self-assembly process might have advantages since the straightforward investigation and manipulation of this process is allowed.

Here, the synthesis of well-defined conjugates comprising cyclic (D-*alt*-L)-peptides and synthetic polymers as well as their self-assembly into nanotubes and further into networks are described. Linear octapeptides are synthesized using solid-phase supported peptide synthesis (SPPS). These linear peptides were cyclized by head-to-tail cyclization in dilute solution. The subsequent conjugation of a carboxylate end-functionalized poly(*n*-butyl acrylate) to the cyclic peptide precursors results in polymer−peptide conjugates (coil−ring−coil) with the capability to aggregate into tubular structures.

Experimental Section

Materials. 2-Bromopropionic acid (Aldrich, 99+%), *n*-butyl acrylate (*n*BA, Aldrich, 99%), and *N*,*N*-dimethylformamide (DMF; Aldrich, 99+%) were distilled and stored at −15 °C. Diisopropylethylamine (DIPEA; Acros, peptide grade), piperidine (Acros, peptide grade), *N*,*N*,*N*′,*N*′,*N*″-pentamethyldiethylenetriamine (PMDETA; Aldrich, 99%), trifluoracetic acid (TFA; Acros, peptide grade), 1-Ethyl-3-(3-dimethyllaminopropyl)carbodiimide hydrochloride (EDC; Fluka, 99%) and 1-methylimidazole (NMI; Fluka, 99+%) have been applied as received. Copper(I) bromide (CuBr; Aldrich, 98%) was purified according to standard procedure.[43] All other reagents were used as received from Aldrich. 9-Fluorenmethoxycarbonyl (Fmoc) amino acid derivatives (Fmoc-L-Gln(*t*Bu)-OH, Fmoc-D-Ala-OH·H_2O, Fmoc-L-Lys(Boc)-OH), polystyrene-(2-chlorotrityl) resin (loading: 1.5 mmol/g), and 2-(1*H*-benzotriazole-1-yl)-1,1,3,3-tetramethyluronium hexafluorophosphate (HBTU) (IRIS Biotech GmbH, Germany) were used as received. 2-(1*H*-7-Azabenzotriazol-1-yl)-1,1,3,3-tetramethyl uronium hexafluorophosphate (HATU) and 1-hydroxy-7-azabenzotriazole (HOAT) were received form Applied Biosystems (ABI Darmstadt, Germany). Benzyl 2-bromopropionate was synthesized according to established procedures.[44]

Instrumentation. The synthesis of the linear oligopeptide was performed on an Applied Biosystems ABI 433a peptide synthesizer. Mass spectrometry was performed on a high performance liquid chromatograph electron spray ionization mass spectrometer (LC−ESI−MS) (Shimadzu, qp8000α, Duisburg, Germany). Nuclear magnetic resonance spectra (NMR) were recorded on a Bruker DPX-400 spectrometer at 400.1 MHz. Dynamic light scattering (DLS) measurements were carried out using a standard, laboratory-built scattering spectrometer operating at 633 or 488 nm (Argon-Ions-Laser, Firma Coherent, model Innova 300) (power: 30−600 mW). The initial experiments were performed at 90° scattering angle. High quality of the scattering curves was ensured by repeating measurements several times. The radius-distribution of the aggregates in solution was calculated from the experimental correlation functions using the program FASTORT.EXE131.[45] IR spectra were recorded on a BioRad 6000 FT-IR. The samples were measured in the solid state using a Single Reflection Diamond ATR. AFM was performed on a NanoScope IIIa microscope (Digital Instruments) with a 10×10 μm e-scanner and silicon tips (type NCR-W; tip radius < 10 nm, spring constant of 42 N m^{-1} at a resonance frequency of 285 kHz). All measurements were carried out in tapping mode. The analyses of the aggregate dimensions were carried out on a sample exhibiting separated structures by averaging over at least 30 values. TEM micrographs were obtained with a Zeiss EM 912 OMEGA instrument operating at an acceleration voltage of 120 kV. The diluted aggregate solutions in THF were placed on a 400-mesh carbon-coated copper grid, and after 10 s, the solvent was removed with a filter paper.

Synthesis of the Linear Octapeptide (L-Gln(Trt)-D-Ala-L-Lys-(Boc)-D-Ala)$_2$ (II). 2-Chlorotrityl chloride resin (1.5 g, 1.5 mmol/g) was placed in a batch reactor and suspended in DCM (12 mL). The suspension was shaken for 5 min and the solvent was filtered off. Fmoc-L-Gln(Trt)-OH (1.83 g, 3.0 mmol) in DCM (10 mL) and DIPEA (1.0 mL, 7.1 mmol) were added and the suspension was shaken for 60 min at room temperature. The solvents were filtered off and the resin was washed with DMF (2 × 2 min). A mixture of DCM/MeOH/DIPEA (80:15:5) (10 mL) was added to the resin. The resin was shaken for 10 min and solvents were filtered off. This procedure was repeated once more after which the resin was washed with DMF (3 × 10 mL), methanol (3 × 10 mL), and DCM (3 × 10 mL). The preloaded resin (**I**) was dried in vacuo and used for further solid-phase supported peptide synthesis at the peptide synthesizer with *N*-methyl-2-pyrrolidone (NMP) as solvent. Standard FastMoc synthesis protocols were applied (including double coupling and end-capping procedures) and the amino acid coupling was facilitated by HBTU/DIPEA.[46] After final Fmoc group removal, the product was cleaved manually with 2% TFA in DCM (2 × 10 mL; 1 min) and the resin was washed with DCM (10 mL). The fractions were added to dioxane (50 mL) and the product was concentrated to a white solid, redisolved in MeOH (8−10 mL) and precipitated in diethyl ether (30 mL). The product was freeze-dried from MeOH/dioxane (1:1), resulting in 1.87 g (1.25 mmol) of octapeptide **II** as a white powder.

^{1}H NMR (DMSO-d_6): δ = 8.60 (d, 2H, NH), 8.52 (d, 1H, NH), 8.35 (d, 1H, NH), 8.13 (d, 1H, NH), 8.06 (d, 2H, NH), 7.94 (d, 1H, NH), 7.24−7.20 (m, 12H, Trt), 7.16−7.11 (m, 18H, Trt), 6.70 (m, 2H, NH), 4.40−4.10 (m, 8H, CH), 2.83 (m, 4H, CH_2), 2.30−2.20 (m, 4H, CH_2), 1.91−1.75 (m, 2H, CH_2), 1.72−1.53 (m, 4H, CH_2), 1.53−1.40 (m, 2H, CH_2), 1.32 (s, 18H, *t*Boc), 1.28 (d, 3H, CH_3), 1.40−1.10 (m, 8H, CH_2), 1.22−1.11 (m, 9H, CH_3) ppm. ^{13}C NMR (DMSO-d_6): δ = 173.7, 172.6, 172.5, 172.0, 171.6, 171.5, 171.4, 170.0, 158.7, 158.3, 155.9, 145.2, 128.9, 127.8, 126.7, 77.7,

69.6, 66.7, 52.7, 52.6, 52.5, 51.8, 49.0, 48.8, 48.6, 48.42, 32.7, 32.6, 32.2, 29.4, 28.6, 28.3, 27.6, 22.9, 19.3, 18.8, 17.8 ppm. ESI−MS: *m*/*z* (%) = 1257 (14) $[M - Trt + H]^+$, 1499 (100) $[M + H]^+$, 1522 (5) $[M + Na]^+$.

Synthesis of the Cyclic Octapeptide (L-Gln-D-Ala-L-Lys-D-Ala)$_2$ (III). An oven dried 2 L flask equipped with a magnetic stir bar was charged with linear peptide **II** (1.6 g, 1.07 mmol). The linear peptide was dissolved in DMF (900 mL). The flask cooled to 0 °C with an ice-bath, under positive Argon pressure. HATU and HOAt in DMF (100 mL) were added. After subsequent addition of DIPEA the solution was left for 3 h at 0 °C. The mixture was concentrated under reduced pressure to about 20 mL (white milky solution) and added to MeOH (30 mL). The precipitate was washed multiple times with MeOH and freeze-dried from dioxane/benzene (1:1), resulting in 1.37 g (87%) of protected **III** as white powder.

From a part of the cyclic peptide, the Trt and *t*Bu protection groups were cleaved. Therefore, 530 mg of the product was placed in a 10 mL Schlenk flask. Then 8 mL of the cleavage cocktail TFA/DCM/TES (48:50:2) was added and the solution was stirred at room temperature for 1.5 h. The solution was concentrated in vacuo to ∼2 mL, and the product was precipitated in methanol (10 mL), washed with diethyl ether (10 mL), acetonitrile (20 mL) and freeze-dried from acetonitrile/benzene 1:1, resulting in 282 mg (98%) of **III** as a white fluffy powder.

^{1}H NMR(DMSO-d_6): δ = 8.30−7.50 (m, 8H, NH), 4.60−3.90 (m, 8H, CH), 2.90−2.71 (m, 4H, CH_2), 2.20−2.03 (m, 4H, CH_2), 1.95−1.81 (m, 2H, CH_2), 1.80−1.63 (m, 4H, CH_2), 1.61−1.48 (m, 6H, CH_2), 1.46−1.17 (m, 16H, CH_2 & CH_3) ppm. ESI−MS: *m*/*z* (%) = 399 (100) $[M + 2H]^{2+}$, 797 (3.2) $[M + H]^+$, 819 (0.2) $[M + Na]^+$.

Synthesis of Carboxylated Poly(*n*-butyl acrylate) by ATRP. CuBr (718 mg, 5 mmol) and $CuBr_2$ (45 mg, 0.2 mmol) were placed into a Schlenk flask, which was purged with argon. A degassed solution of *n*BA (28.7 mL, 200 mmol) and PMDETA (1.1 mL, 5.2 mmol) in acetonitrile (11 mL) was added via syringe transfer under inert gas atmosphere. The reaction mixture was stirred for 1 h at room temperature to allow the formation of the copper complex and subsequently preheated to 60 °C. The polymerization was initiated by the addition of a degassed solution of benzyl 2-bromopropionate (1.75 mL, 10 mmol) in acetonitrile (2 mL). After 2 h, the polymerization was stopped by cooling the mixture to room temperature and exposing it to air. After evaporation of the solvent and the residual monomer under high vacuum, the mixture was diluted with acetone and filtered through an alumina column to remove the catalyst, and the polymer was precipitated in aqueous methanol (20 vol % water) to yield the precursor polymer (17.2 g, 82%). The benzyl ester group was selectively cleaved under reductive conditions (ammonium formiate, Pd/C (10 wt %) in absolute ethanol) giving P*n*BA-COOH as a clear colorless oil (yield 75%) after reprecipitation in aqueous methanol (15 vol % water).

^{1}H NMR ($CDCl_3$): δ = 4.05 (b, 32 H, OCH_2), 2.28 (b, 16 H, CH), 1.59−1.91 (b, 64 H, CH_2), 1.36−1.38 (b, 32 H, CH_2), 1.18 (d, 3 H, CH_3), 0.93 (t, 46 H, CH_3) ppm. ^{13}C NMR (DMSO-d_6); δ = 171.6, 72.4, 60.3, 46.2, 44.6, 35.6, 30.7, 27.7, 26.2, 22.8 ppm. FT-IR: ν (cm^{-1}): 2960−2874 (s, C−H), 1734 (s, C═O), 1166 (w, O−H); MALDI−TOF−MS: 2 homologous series with 128 Da mass of the repeat units, each ($m/z_{(max\ intensity)}$ = 2035.8 and 2019.8, which can be assigned to $[M + K]^+$ and $[M + Na]^+$, respectively with 16 *n*BA repeat units and an end group mass of 74.1 Da (propionic acid)); GPC: (THF, p*n*BA-standards) M_n = 2100 g/mol, DP_n = 16, M_w/M_n = 1.10.

Synthesis of *cyc*[(L-Gln-D-Ala-L-Lys-D-Ala)$_2$]-(P*n*BA)$_2$ Conjugate (IV). The cyclic peptide **III** (120 mg, 0.15 mmol) was dissolved in dry DMF (10 mL). P*n*BA-COOH (900 mg, 0.45 mmol) in DMF (3 mL) was added and the solution was degassed with Argon. A solution of EDC (172 mg, 0.9 mmol) and DIPEA (0.35 mL, 2.0 mmol) in DMF (3 mL) was injected, and the reaction mixture was stirred overnight at room temperature. The solution was concentrated, MeOH (20 mL) and water (30 mL) were added and the product was centrifuged off. After reprecipitation in diethyl ether/methanol the product **III** was freeze-dried from benzene/acetonitrile (1:1) and isolated as a sticky white solid.

^{1}H NMR(DMF-d_7): δ = 8.30−6.70 (m, NH), 4.20−4.00 (m, 64H, OCH_2), 2.55−2.25 (m, 36H, CH&CH_2), 2.15−2.02 (m, 4H, CH_2), 1.95−1.85 (m, 16H, CH_2), 1.80−1.30 (m, 180H, CH_2), 1.20−1.08 (m, 12H, CH_3), 1.08−0.85 (m, 96H, CH_3) ppm.

Results and Discussion

The combination of the structural and functional control of sequence defined polypeptides with the diversity and stability of synthetic polymers in peptide−polymer conjugates potentially result in biohybrid materials that may actively interface biological and synthetic systems. Particularly, the cyclic (D-*alt*-L)-peptides are interesting because of their rigidity and shape persistency. This allows the geometry fixation and positioning of functionalities, analogue to synthetic systems[23] but unlike, e.g., crown ethers or cycloalkanes.[23, 47]

To conjugate a synthetic polymer to such cyclic (D-*alt*-L)-peptides, a coupling approach was applied. For this a polymer exhibiting a carboxylic acid end group functionality was attached to the ϵ-amine group of lysine residues appropriately positioned in the preformed peptide cycle (Scheme 1). The direct coupling approach allows for the straightforward analysis of the precursor compounds (polymer and peptide cycle), and hence, ensures the controlled synthesis of the conjugate. Ensuring ease of analysis of the conjugates by choosing the appropriate synthetic approach is important, because the analysis of peptide−polymer conjugates showing high tendency to aggregate remains demanding.

Following the approach outlined in Figure 1, a linear precursor for the peptide cycle was synthesized. This (D-*alt*-L)-α-octapeptide exhibits the H−(L-Gln(Trt)-D-Ala-L-Lys(*t*Boc)-D-Ala)$_2$−OH sequence (Scheme 1, **II**). After head to tail cyclization, a (D-*alt*-L)-peptide cycle **III** was obtained in which the symmetry as well as functional analogy to systems described by Ghardiri et al. has been preserved, ensuring the aggregation potential of the peptide ring.[14,27] While the D-alanine moieties generate lipophilicity, without producing steric hindrance, the L-lysines as well as the L-glutamines enhance the solubility. The alternating combination of alanine and functional amino acid residues encodes a peptide cycle that has been proven to self-assemble, providing high aggregation tendency but preserving aggregation dynamics.[22] The L-lysines positioned at the opposite sides of the peptide ring provides anchor functionalities for attachment of the polymer segments, while the L-glutamine side chain functionalities could potentially form hydrogen bonds, modulating the lateral contact between neighboring peptide tubes.[22] The latter depends, however, on steric shielding by the polymer segments.

The linear (D-*alt*-L)-α-octapeptide (**II**) was synthesized by applying solid-phase supported peptide synthesis (SPPS) techniques and sequential attachment of Fmoc amino acid derivatives, assembling the peptide sequence as outlined in Scheme 1.[46] The applied resin (**I**) had an acid labile 2-chlorotrityl linker, allowing the liberation of the fully protected, linear peptide **II** from the support after peptide synthesis. The cleavage of **II** from the resin without removing the side chain protecting groups (trityl of Gln and the *tert*-butyl oxycarbonyl (*t*Boc) of Lys) was accomplished by the treatment of the resin with 2 vol % TFA in DCM. After precipitating the peptide in diethyl ether and freeze-drying, the clean formation of the linear analogue **II** was confirmed by ESI−MS (Figure 2a) by showing the corresponding mass signals for the different ion adducts (*m*/*z* 1499 ($[M + H]^+$) and 1522 ($[M + Na]^+$)). No evidence could be found for the formation of side products such as, e.g., deletion sequences.

Scheme 1. Synthesis of the Conjugate from Poly(*n*-butyl acrylates) and Cyclic (D-*alt*-L)-α-Octapeptide (IV)[a]

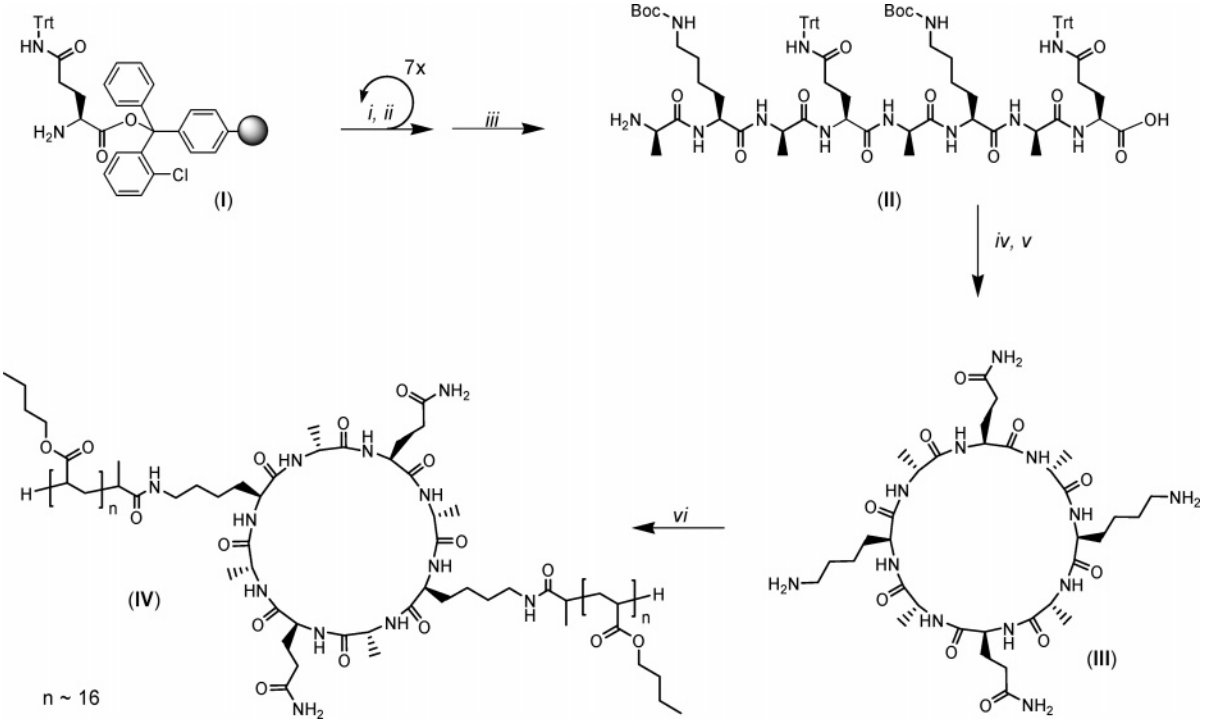

[a] Reagents and conditions: (i) Fmoc-AA-OH, HBTU, DIPEA, NMP; (ii) 20 vol % piperidine, NMP; (iii) 2% TFA in DCM; (iv) HATU, HOAt, DIPEA, DMF, 0 °C, 3 h, 1 mM peptide solvent; (v) TES/TFA/DCM (1:24:25); (vi) poly(*n*-butyl acrylate) carboxylic acid, EDAC·HCl, DIPEA, DMF.

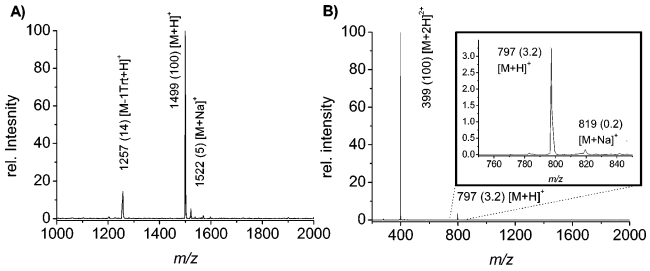

Figure 2. ESI−MS spectrum of linear (D-*alt*-L)-α-octapeptide **II** (a) and cyclic (D-*alt*-L)-α-octapeptide **III** (b).

Perhaps even more important than this was the absence of signals corresponding to (partially) deprotected side chain functionalities of lysine because this would cause side reactions during the cyclization step.

Moreover, the qualitative MS results could be supported by ^{1}H NMR measurements. The comparison of the integral intensity ratios of the spectrum of **II** verifies on one hand that each amino acid is present in the expected ratio of 2:4:2 for Gln:Ala:Lys and on the other hand that no loss of *t*Boc or Trt protecting groups took place. This verifies a clean product formation, making further chromatographic purification unnecessary and allowing the direct transformation of the linear precursor **II** into the peptide cycle **III**.

A head-to-tail cyclization of **II** was performed applying high dilution conditions in DMF (c[**II**] = 1.0 mM) using rather enforced coupling conditions with HATU and HOAt as activators. The self-organization tendency of the cyclic peptides compared to the linear analogues could be exploited to conveniently purify the cyclization mixture. This avoids time and material consuming HPLC purification steps and allows gram scale reactions. During partial evaporation of the solvent, the cyclic peptides precipitate cleanly from solution, while the linear analogue remains in solution. This already highlighted the strong tendency of the ring structure to form aggregates compared to the linear analogue. The product was reprecipitated in methanol to ensure the quantitative removal of the linear precursor allowing the isolation of about 1.4 g of (D-*alt*-L)-peptide cycles (87% yield). The chemical identity of **III** was verified by means of MS and NMR after removal of the side chain protecting groups, using TFA/DCM/TES (50:48:2). The deprotected product was isolated by precipitation in methanol, subsequently washing with diethyl ether, acetonitrile and freeze-dried from acetonitrile/benzene. ESI−MS confirmed the formation of **III** (Figure 2b) by showing the corresponding mass signals for the different ion adducts (m/z 399 $[M + 2H]^{2+}$, 797 $[M + H]^+$, and 819 $[M + Na]^+$). Furthermore, the quantitative removal of the side chain protecting groups (*t*Boc and trt from the Lys and Gln, respectively) was suggested by ^{1}H NMR spectroscopy, showing the absence of both resonances around δ = 7.24−7.20 and 1.32 ppm for Trt and *t*Boc, respectively.

To obtain the peptide−polymer conjugate, an end group functionalized poly(*n*-butyl acrylate) (p*n*BA) block was attached in solution to the ϵ-amine groups of the lysine residues of the cyclic peptide (Scheme 1). For that a p*n*BA, exhibiting only one terminal carboxylate functionality was synthesized via atom transfer radical polymerization (ATRP). A selective introduction of the end-functionality could be achieved by the application of benzyl 2-bromopropionate as a functional ATRP-initiator. The benzyl ester group was selectively cleaved via reductive means, preventing a saponification of the acrylate ester moieties. Furthermore, under these conditions the α-bromo functionality of the polymer is removed, which otherwise might cause side reactions during conjugation. The resulting p*n*BA with carboxylic acid end group was characterized by gel permeations chromatography showing a M_n = 2100 (DP_n = 16) and M_w/M_n = 1.10. The selective end-functionalization was verified by ^{1}H NMR spectroscopy proving the absence of the characteristic resonances for the benzyl ester group (cf. Supporting Informa-

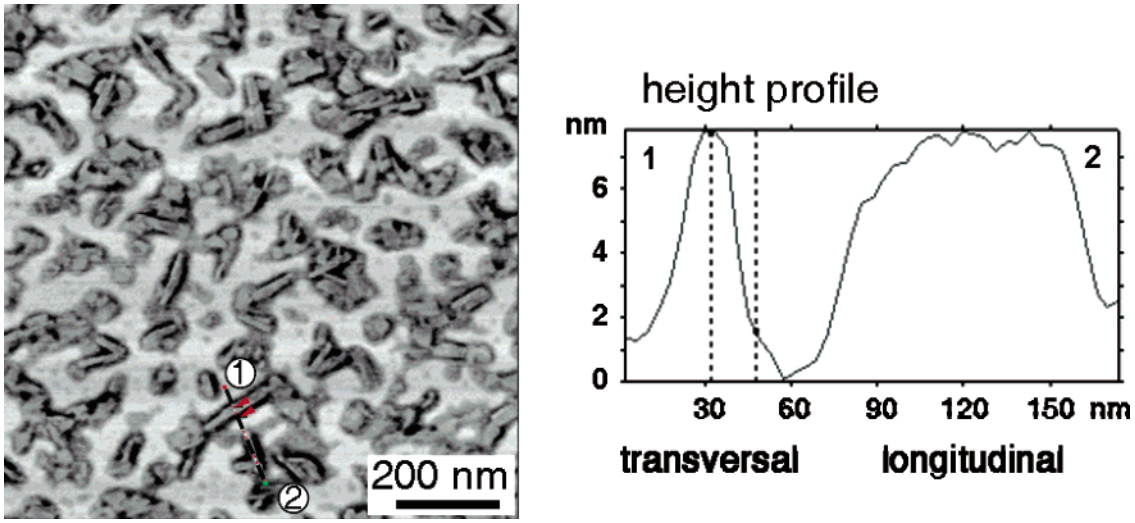

Figure 3. AFM images of the nanotubes formed by **IV** in DMF (0.1 mg/mL) deposited onto mica substrate. phase $z = 30°$ (corresponding height profile from topology mode).

tion). Moreover, only one homologues row could be observed in MALDI−TOF−MS, which was assignable to the expected structure within ±1 Da accuracy.

The conjugation of two p*n*BAs to the ϵ-amino groups of the lysine residues positioned at opposite sides of the ring was established using mild coupling protocols with EDAC as activator in DMF (Scheme 1).[46] The p*n*BA−ring−p*n*BA conjugate **IV** could be isolated after multiple times reprecipitation in diethyl ether/methanol, as a good solvent for low molecular weight p*n*BA and subsequently freeze-drying from benzene/acetonitrile. The successful attachment of the polymer chains to the cyclic (D-*alt*-L)-α-octapeptide was confirmed by ^{1}H NMR spectroscopy.

Therefore, the integral intensity of the resonances characteristic for the polymer block ($\delta = 4.20-4.00$ ppm (OCH_2)) was compared with that of the methyl groups of the alanine ($\delta = 1.20-1.08$ ppm (CH_3)) representative for the peptide segment. This shows a ratio of 4 alanine residues to about 32 *n*BA repeating units, meeting the expected value within the experimental error and, hence, suggesting that two polymer chains are attached to the cyclic (D-*alt*-L)-peptide.

To obtain well-defined aggregates it has been demonstrated that assays which combine careful deaggregation/denaturation with successively controlled reaggregation were most suitable, because kinetically stable assemblies with their free energy in a local minimum can be avoided.[8]

Therefore, the deaggregation of **IV** in diverse solvents was investigated by dynamic light scattering (DLS) (cf. Supporting Information). However, independently of the used solvents, such as $CHCl_3$, THF or DMF, DLS suggested the formation of stable aggregates with hydrodynamic radii ranging from $R_h = 37$ to 49 nm. Additionally, thermal treatment could not dramatically influence the dissociation process of the aggregates, because similar R_h's were obtained within each solvent, by either heating the samples for 1 h prior to the measurements (e.g., 60 °C for $CHCl_3$, and THF and 100 °C for DMF) or during the measurements (e.g., 80 °C for DMF). These results show that stable aggregates are formed and that strong competitive solvents, such as DMF are not able to effectively disassemble the aggregates, even at increased temperatures. This highlights the enormous aggregation potential of the (D-*alt*-L)-cyclopeptides for the peptide-guided organization of synthetic polymers.

To investigate the solution structures in more detail, microscopy studies were performed allowing the direct visualization of their morphology. Tapping mode atomic force microscopy (AFM) was used to analyze the self-assembly behavior of **IV**. In the case of a dynamic aggregation process it was expected that the actual morphology will depend on the employed solvent. Thus, a series of solutions of **IV** in $CHCl_3$, THF and DMF (1 mg/mL) were prepared and spin-coated onto mica substrates. Figure 3 shows the AFM micrograph of deposited aggregates from DMF solution as a representative sample for all other solvents, indicating kinetically frozen aggregates.

The AFM micrograph shows rodlike structures with an average height of about 7 ± 2 nm and lengths of up to 180 nm. The anisometry of the structures gives initial indications that the aggregate formation is driven by peptide organization. This is supported by FT-IR measurement of thin films of **IV**, showing the amide I vibration bands at $\upsilon = 1626$ and 1692 cm^{-1} and amide II vibration band at $\upsilon = 1540$ cm^{-1} that are characteristic for antiparallel β-sheets present in aggregates of (D-*alt*-L)-cyclopeptides.[22] However, the large height value of the structures, combined with no conclusive evidence for a distinct inner structure (Figure 3) allows only the speculation that the aggregates might consist of bundles of multiple, smaller protostructures, because the diameter of a peptide cycle is about 1.4 nm.[48] It is noteworthy that no lateral interactions can be observed between the objects, as indicated by AFM, showing that the rod structures apparently have no tendency to align parallel.

The data presented above indicate that the formation of aggregates occur already prior to addition of the different solvents and remains kinetically frozen under these conditions. The aggregation probably takes place during the precipitation of **IV** after the synthesis, as supported by FT-IR measurements of solid **IV**, showing similar characteristic amide I adsorption bands for the β-sheet structure motif.

To avoid pre-aggregation of **IV** under kinetic conditions, the complete dissociation of the aggregates has to be ensured. This was finally achieved by the treatment of **IV** with TFA (100%), resulting in the absence of any organized structure, as could be confirmed by AFM (see Supporting Information).

After removal of the TFA at room temperature, **IV** was redissolved in a small amount of DMF and further diluted with THF (final c[**IV**] = 0.04 and 0.004 mg/mL; DMF = 0.4 and 0.04 vol %, respectively). The addition of THF results in the decrease in H-bond acceptor properties of the solvent and hence triggers the aggregation process. This was obvious because AFM micrographs obtained from spin-coating the solutions onto a

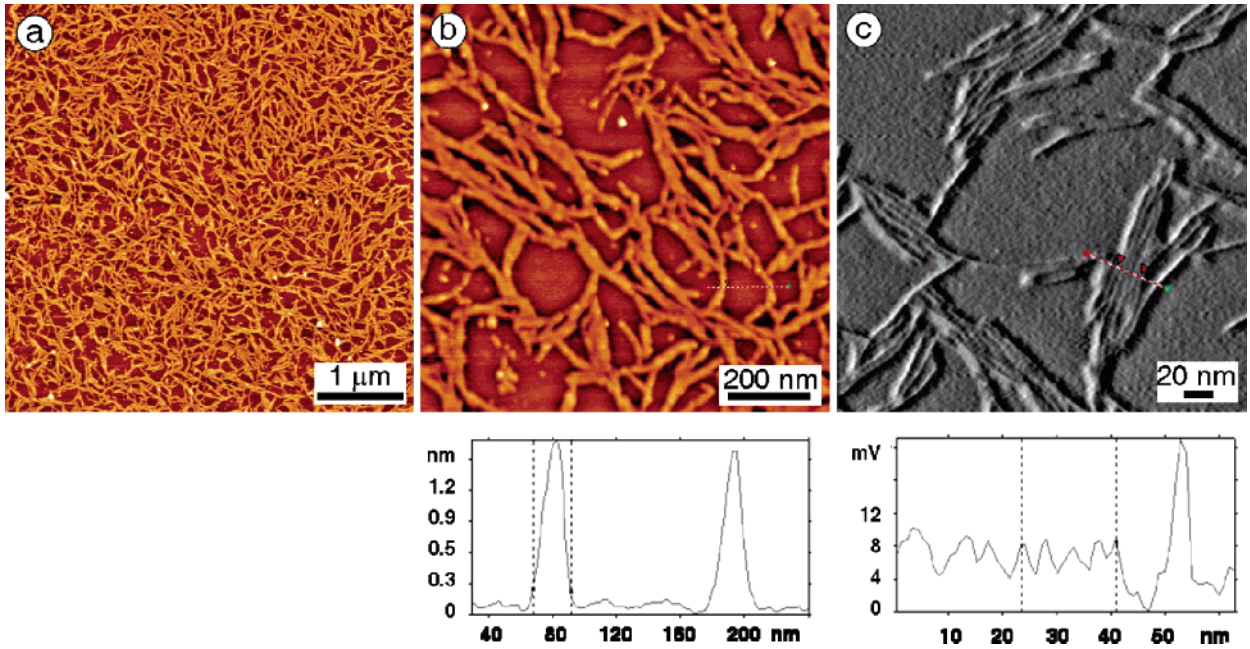

Figure 4. AFM images of the nanotubes formed by **IV** deposited onto mica substrate after treatment with TFA and reassembly in DMF/THF: (a, b) height, $z = 3$ nm, [**IV**] = 0.04 mg/mL; (c) high-resolution AFM image, amplitude $z = 25$ mV, [**IV**] = 0.004 mg/mL.

mica substrate show the formation of extended fiber networks (Figure 4a, b). These are composed of fiberlike aggregates (Figure 4c) with an average height of about 1.4 ± 0.2 nm and widths of about 4.8 ± 0.3 nm. The latter could be accessed from high resolution AFM of densely packed fiber bundles by measuring the distances of maxima in the amplitude imaging mode (Figure 4c). This periodicity was confirmed with less accuracy by evaluating the histograms of the corresponding height image (5.0 ± 0.8 nm). However, the viscoelastic contrast is superior to the topological structure differences. The length of the fiber aggregates is highly polydisperse and a maximum length could be roughly estimated with 200−300 nm. However, the obvious tendency of the fibers to form bundles makes the exact determination difficult.

To exclude that the formation of the fiberlike aggregates and further assembly of these structures to networks has been induced by the high energy surface of the mica substrate, the same solution used for AFM sample preparation was deposited on a carbon coated grid for transmission electron microscopy (TEM). Similar network structures could be observed with TEM on a substrate with completely different surface energies, suggesting that the observed networks are already present within the solution (Figure 5). However, the peptide and the polymer exhibit neither good contrast from the background, nor sufficiently different chemical properties to allow selective staining. As a consequence, setting the appropriate focus is difficult, leading to a micrograph with rather limited resolution and making it difficult to access reliable dimensions.

However, selected area electron diffraction (SAED) allows to verify that the cyclic (D-*alt*-L)-peptide segments adopt a β-sheet structure motif, because periodicities of 4.63 Å were measured (see Figure 5, inset). This intersubunit distance is in agreement with previously reported *d* spacings for cyclic (D-*alt*-L)-peptides in tightly hydrogen bonded ring-stacks.[22] Moreover this is consistent with FT-IR measurements, showing the typical amide I adsorption bands at $\upsilon = 1632$ and 1672 cm^{-1}.[22]

Considering the dimensions of the observed structures and the self-assembly behavior of peptide−polymer conjugates,[8,9,39] of cyclic (D-*alt*-L)-peptides,[22] and of coil−ring−coil polymers,[23,49] a preliminary structure model can be suggested, as

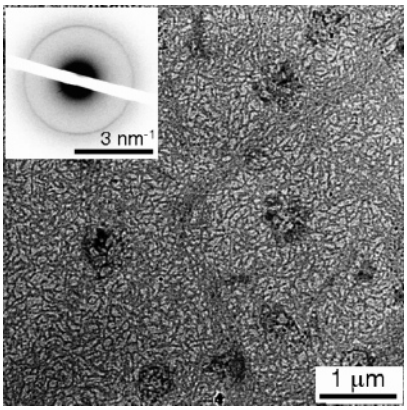

Figure 5. TEM image of the fiber network formed by **IV** (0.004 mg/mL) after staining with uranyl acetate. Inset: selected area electron diffraction micrograph.

outlined in Figure 6. Because of the strong restriction in self-assembly modes of cyclic (D-*alt*-L)-peptides, a tubular structure via stacking of planar peptide rings is most likely (see Figure 6a). The suggested peptide organization principle meets the spectroscopic (FT-IR) and scattering (SAED) results, since the rings are formed by peptide β-strands and the stacked rings are stabilized by inter-ring H-bonding of the peptides adopting an antiparallel β-sheet. The organization of the p*n*BA blocks of the conjugates is facilitated by the peptide self-assembly process, and hence, the formation of a tubular core−shell structure is likely (Figure 6, parts b and c). The model in which the polymer wraps around a hollow peptide tube (Figure 6b) was confirmed by high-resolution AFM imaging, showing a core and a shell with distinct different viscoelastic properties (Figure 4c).

The diameter of the structures in solution can be calculated with about 4.0 nm, assuming the diameter of cyclic (D-*alt*-L)-α-octapeptides of 1.4 nm [48] and two p*n*BA blocks adapting a statistical coil configuration.

Considering that the core−shell structures are deposited on mica substrate, the observed structure height of 1.4 ± 0.2 nm meets accurately the height of a naked peptide tube. This indicates that the p*n*BA chains apparently avoid back-folding

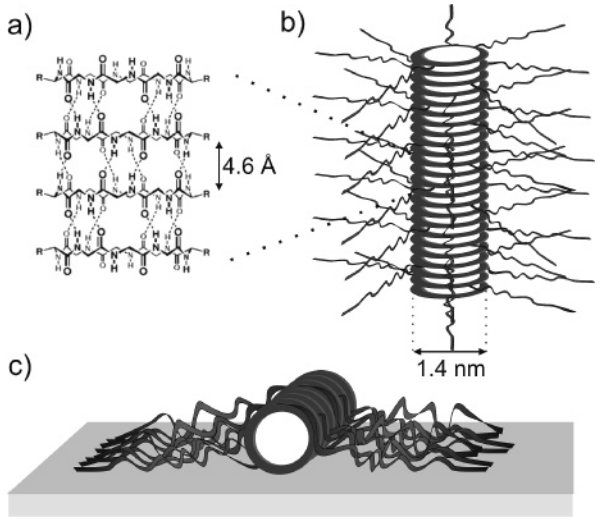

Figure 6. Schematically illustration of the nanotubes self-assembled from polymer−peptide−polymer ABA-conjugates from poly(*n*-butyl acrylates) and cyclic (D-*alt*-L)-α-octapeptides **IV** (a), in solution (b), and on a mica surface (c).

onto the peptide tube structure. Such behavior is expected, because p*n*BA interacts strongly with mica, as has been described e.g. for molecular bottlebrushes with p*n*BA side chains.[43] Hence a maximization of p*n*BA-mica contacts is most likely that additionally explains the increased width of the supported structures (5 nm) compared to the calculated diameter of the solution structures (4 nm). Since the p*n*BA blocks adsorb strongly to the mica substrate, an extension of the polymer coils is likely (Figure 6c). However, the packing constraints are not sufficient to lead to a fully extended, brush configuration, which would result in a 2-dimensional bottle brush structure of about 9.4 nm width. The attempt to support this hypothesis by investigating the structures on carbon or silica supports that show less significant interactions with p*n*BA failed, because the objects are shifted during the AFM scanning process, leading to fuzzy images that prevent the determination of an exact width.

It is noteworthy that the polymer−peptide fiber tubes show further organization, forming networks as evident by both AFM and TEM investigations (Figures 4 and 5). Network formation indicates the capability of proto-structures to interact laterally. These interactions probably result on one hand from the entanglement of p*n*BA side chains or on the other hand from intertubular hydrogen-bonds between the glutamine side chains. The latter was described previously for peptide nanotubes formed by cyclic (D-*alt*-L)-peptides, suggesting intertubular glutamine-glutamine hydrogen-bond contacts to induce long-range order in such aggregates.[22] However, these interactions appears to be rather weak at the concentration of 0.04 mg/mL and does not result in the formation of continuous organo-gel, by showing a fluid−gel transition. Probably, this could be the result of either very soft interactions between the fiber tubes or an average fiber length that is below the critical length.

Conclusions

In summary, the synthesis and self-assembly behavior of a coil−ring−coil bioconjugate comprising, a cyclic (D-*alt*-L)-α-octapeptide and two poly(*n*-butyl acrylate) blocks has been described.

The polymer−peptide conjugate was synthesized on a gram scale, by solution coupling of a carboxyl end functionalized p*n*BA to a preformed (D-*alt*-L)-cyclopeptide. The latter was accessed by the solid-phase supported peptide synthesis (SPPS) followed by head-to-tail cyclization in solution, applying high dilution conditions. The peptide cycle contained two lysine residues that were positioned at opposite sides in the ring, providing the ϵ-amine functionalities to anchor the p*n*BA blocks. These were accessed separately via atom transfer radical polymerization (ATRP), using a functional initiator and protecting group strategies to selectively introduce the carboxyl end-functionality necessary for the peptide conjugation. It was demonstrated, that the coupling approach, involving separate synthesis of both well-defined polymer and cyclopeptide followed by the coupling of these precursors ensure the controlled synthesis and ease of analysis of the conjugate.

The self-assembly properties described for unsubstituted (D-*alt*-L)-cyclopeptides were not dramatically altered by the conjugation of two polymer blocks. Thus, the coil−ring−coil conjugate exhibited a strong tendency to form uniform tubelike structures. Atomic force microscopy (AFM) showed that these aggregates deposited on mica substrate, have an average height of about 1.4 ± 0.2 nm, a width of 5 nm and roughly estimated lengths of up to 200−300 nm. A structure model has been suggested comprising a tubular peptide core build via stacking of cyclopeptides and a polymer shell wrapping around this hollow tube. This model is consistent with the observed structure dimensions and the spectroscopic as well as scattering investigations (infrared spectroscopy and electron diffraction, respectively). The latter verifies that the cyclopeptides adopting a β-sheet secondary structure, which stabilizes the stacks of rings along the fiber growth axis by H-bond formation.

The tubelike structures organize further into fiber networks as evidenced by both AFM and transmission electron microscopy (TEM). This indicates the ability of the proto-structures to interact laterally, probably as a result of entanglement of the p*n*BA side chains or from intertubular hydrogen-bonds between side chain functionalities of amino acid moieties (L-glutamine).

The resulting peptide−polymer nanotubes possess a functionalizable exterior and a hollow interior that allows only a passive transport of substrates, depending on the ring size of the cyclopeptides. However, for recognition, selective or even active transport purposes it is essential to functionalize the interior of the conjugate nanotubes. Therefore, ongoing research in our laboratories focuses on the design of conjugates combining polymers with cyclopeptides that carry unnatural amino acids, allowing to access polymer−peptide tubes with orthogonal addressable internal and external functionalities.

Acknowledgment. Prof. Jürgen Rabe (Humboldt University, Berlin), Jens Hentschel, Hartmut Rettig, Anne Heilig, Arne Thomas, Katharina Ostwald, Jessica Brandt, Marlies Gräwert, and Olaf Niemeyer are thanked for the contributions to this project. Financial support was received from the German Research Foundation (DFG) through the Emmy Noether Program (BO 1762/2-2) and the Max Planck Society.

Supporting Information Available: Figures showing NMR spectra of the end-functionalized poly(*n*-butyl acrylate) prior to and after the deprotection, DLS data of **IV** in different solvents (prior to the deaggregation), and an AFM image of the deaggregated **IV** in 100% TFA. This material is available free of charge via the Internet at http://pubs.acs.org.

References and Notes

(1) Burkoth, T. S.; Benzinger, T. L. S.; Urban, V.; Lynn, D. G.; Meredith, S. C.; Thiyagarajan, P. *J. Am. Chem. Soc.* **1999**, *121*, 7429.
(2) Rathore, O.; Sogah, D. Y. *J. Am. Chem. Soc.* **2001**, *123*, 5231.
(3) Vandermeulen, G. W. M.; Tziatzios, C.; Klok, H. A. *Macromolecules* **2003**, *36*, 4107.

(4) Ayres, L.; Vos, M. R. J.; Adams, P.; Shklyarevskiy, I. O.; van Hest, J. C. M. *Macromolecules* **2003**, *36*, 5967.
(5) Rosler, A.; Klok, H. A.; Hamley, I. W.; Castelletto, V.; Mykhaylyk, O. O. *Biomacromolecules* **2003**, *4*, 859.
(6) Smeenk, J. M.; Otten, M. B. J.; Thies, J.; Tirrell, D. A.; Stunnenberg, H. G.; van Hest, J. C. M. *Angew. Chem., Int. Ed.* **2005**, *44*, 1968.
(7) Collier, J. H.; Messersmith, P. B. *Adv. Mater.* **2004**, *16*, 907.
(8) Eckhardt, D.; Groenewolt, M.; Krause, E.; Börner, H. G. *Chem. Commun.* **2005**, 2814.
(9) Hentschel, J.; Krause, E.; G.; B. H. *J. Am. Chem. Soc.* **2006**, *128*, 7722.
(10) Jun, H. W.; Paramonov, S. E.; Hartgerink, J. D. *Soft Matter* **2006**, *2*, 177.
(11) Lamm, M. S.; Rajagopal, K.; Schneider, J. P.; Pochan, D. J. *J. Am. Chem. Soc.* **2005**, *127*, 16692.
(12) Pandya, M. J.; Spooner, G. M.; Sunde, M.; Thorpe, J. R.; Rodger, A.; Woolfson, D. N. *Biochemistry* **2000**, *39*, 8728.
(13) Petka, W. A.; Harden, J. L.; McGrath, K. P.; Wirtz, D.; Tirrell, D. A. *Science* **1998**, *281*, 389.
(14) Ghadiri, M. R.; Granja, J. R.; Milligan, R. A.; McRee, D. E.; Khazanovich, N. *Nature* **1993**, *366*, 324.
(15) Paramonov, S. E.; Jun, H.-W.; Hertgerink, J. D. *J. Am. Chem. Soc.* **2006**, *128*, 7291.
(16) Tirrell, M.; Kokkoli, E.; Biesalski, M. *Surf. Sci.* **2002**, *500*, 61.
(17) Aggeli, A.; Bell, M.; Carrick, L. M.; Fishwick, C. W. G.; Harding, R.; Mawer, P. J.; Radford, S. E.; Strong, A. E.; Boden, N. *J. Am. Chem. Soc.* **2003**, *125*, 9619.
(18) Aggeli, A.; Bell, M.; Boden, N.; Carrick, L. M.; Strong, A. E. *Angew. Chem., Int. Ed.* **2003**, *42*, 5603.
(19) Zhang, S. G. *Biotechn. Adv.* **2002**, *20*, 321.
(20) Lashuel, H. A.; LaBrenz, S. R.; Woo, L.; Serpell, L. C.; Kelly, J. W. *J. Am. Chem. Soc.* **2000**, *122*, 5262.
(21) Aggeli, A.; Bell, M.; Boden, N.; Keen, J. N.; McLeish, T. C. B.; Nyrkova, I.; Radford, S. E.; Semenov, A. *J. Mater. Chem.* **1997**, *7*, 1135.
(22) Hartgerink, J. D.; Granja, J. R.; Milligan, R. A.; Ghadiri, M. R. *J. Am. Chem. Soc.* **1996**, *118*, 43.
(23) Höger, S. *Chem.—Eur. J.* **2004**, *10*, 1320.
(24) Granja, J. R.; Ghadiri, M. R. *J. Am. Chem. Soc.* **1994**, *116*, 10785.
(25) Ghadiri, M. R.; Kobayashi, K.; Granja, J. R.; Chadha, R. K.; McRee, D. E. *Angew. Chem., Int. Ed.* **1995**, *34*, 93.
(26) Sanchez-Quesada, J.; Kim, H. S.; Ghadiri, M. R. *Angew. Chem., Int. Ed.* **2001**, *40*, 2503.
(27) Ghadiri, M. R.; Granja, J. R.; Buehler, L. K. *Nature* **1994**, *369*, 301.
(28) Clark, T. D.; Buehler, L. K.; Ghadiri, M. R. *J. Am. Chem. Soc.* **1998**, *120*, 651.
(29) Horne, W. S.; Stout, C. D.; Ghadiri, M. R. *J. Am. Chem. Soc.* **2003**, *125*, 9372.
(30) Fenniri, H.; Packiarajan, M.; Vidale, K. L.; Sherman, D. M.; Hallenga, K.; Wood, K. V.; Stowell, J. G. *J. Am. Chem. Soc.* **2001**, *123*, 3854.
(31) Bong, D. T.; Clark, T. D.; Granja, J. R.; Ghadiri, M. R. *Angew. Chem., Int. Ed.* **2001**, *40*, 988.
(32) Ranganathan, D.; Lakshmi, C.; Haridas, V.; Gopikumar, M. *Pure Appl. Chem.* **2000**, *72*, 365.
(33) Nelson, J. C.; Saven, J. G.; Moore, J. S.; Wolynes, P. G. *Science* **1997**, *277*, 1793.
(34) Gattuso, G.; Menzer, S.; Nepogodiev, S. A.; Stoddart, J. F.; Williams, D. J. *Angew. Chem., Int. Ed.* **1997**, *36*, 1451.
(35) Venkataraman, D.; Lee, S.; Zhang, J. S.; Moore, J. S. *Nature* **1994**, *371*, 591.
(36) Harada, A.; Li, J.; Kamachi, M. *Nature* **1993**, *364*, 516.
(37) Fernandez-Lopez, S.; Kim, H. S.; Choi, E. C.; Delgado, M.; Granja, J. R.; Khasanov, A.; Kraehenbuehl, K.; Long, G.; Weinberger, D. A.; Wilcoxen, K. M.; Ghadiri, M. R. *Nature* **2001**, *412*, 452.
(38) Motesharei, K.; Ghadiri, M. R. *J. Am. Chem. Soc.* **1997**, *119*, 11306.
(39) Couet, J.; Samule, J. D. J. S.; Kopyshev, A.; Santer, S.; Biesalski, M. *Angew. Chem., Int. Ed.* **2005**, *44*, 3297.
(40) Matyjaszewski, K.; Xia, J. *Chem. Rev.* **2001**, *101*, 2921.
(41) Wang, J. S.; Matyjaszewski, K. *J. Am. Chem. Soc.* **1995**, *117*, 5614.
(42) Sheiko, S. S.; Sun, F. C.; Randall, A.; Shirvanyants, D.; Rubinstein, M.; Lee, H.; Matyjaszewski, K. *Nature* **2006**, *440*, 191.
(43) Boerner, H. G.; Beers, K.; Matyjaszewski, K.; Sheiko, S. S.; Moeller, M. *Macromolecules* **2001**, *34*, 4375.
(44) Cai-Yuan, P.; Lei, T.; De-Cheng, W. *Polym. Sci., Part A: Polym. Chem.* **2001**, *39*, 3062.
(45) Schnablegger, H.; Glatter, O. *Appl. Opt.* **1991**, *30*, 4889.
(46) Chan, W. C.; White, P. D. *Fmoc Solid-Phase Peptide Synthesis (A Practical Approach)*; Oxford University Press: Oxford, U.K., 2000.
(47) *Large Ring Molecules.* Wiley: Chichester, U.K., 1996.
(48) Nakanishi, T.; Okamoto, H.; Nagai, Y.; Takeda, K.; Obataya, I.; Mihara, H.; Azehara, H.; Suzuki, Y.; Mizutani, W.; Furukawa, K.; Torimitsu, K. *Phys. Rev. B* **2002**, *66*, 165417.
(49) Rosselli, S.; Ramminger, A. D.; Wagner, T.; Silier, B.; Wiegand, S.; Haussler, W.; Lieser, G.; Scheumann, V.; Hoger, S. *Angew. Chem., Int. Ed.* **2001**, *40*, 3138.

MA061738P